Resilient Cities and Structures 3 (2024) 65–78

Contents lists available at ScienceDirect

Resilient Cities and Structures

journal homepage: www.elsevier.com/locate/rcns

Full Length Article

Evaluating the role of transportation system in community seismic resilience

Kairui Feng [a,*], Cao Wang [b], Quanwang Li [c]

[a] The National Key Laboratory of Autonomous Intelligent Unmanned Systems, Tongji University, Shanghai 200120, China
[b] School of Civil and Environmental Engineering, University of Technology Sydney, Ultimo, NSW 2007, Australia
[c] Department of Civil Engineering, Tsinghua University, Beijing 100084, China

ARTICLE INFO

Keywords:
Community resilience
Transportation system
Earthquake
Retrofit Strategy

ABSTRACT

The swift recuperation of communities following natural hazards heavily relies on the efficiency of transportation systems, facilitating the timely delivery of vital resources and manpower to reconstruction sites. This paper delves into the pivotal role of transportation systems in aiding the recovery of built environments, proposing an evaluative metric that correlates transportation capacity with the speed of post-earthquake recovery. Focusing on optimizing urban population capacity in the aftermath of earthquakes, the study comprehensively examines the impact of pre-earthquake measures such as enhancing building or bridge seismic performance on post-earthquake urban population capacity. The methodology is demonstrated through an analysis of Beijing's transportation system, elucidating how enhancements to transportation infrastructure fortify the resilience of built environments. Additionally, the concept of a resource supply rate is introduced to gauge the level of logistical support available after an earthquake. This rate tends to decrease when transportation damage is significant or when the demands for repairs overwhelm available resources, indicating a need for retrofitting. Through sensitivity analysis, this study explores how investments in the built environment or logistical systems can increase the resource supply rate, thereby contributing to more resilient urban areas in the face of seismic challenges.

1. Introduction

Natural hazards, including earthquakes and hurricanes, imperil the stability and function of built environments across diverse communities. In response to these threats, the emphasis on community resilience has amplified, garnering substantial attention and validation from both academic and policy-making sectors [1]. This has resulted in extensive efforts to both define and quantify community resilience, with a focal aim of pinpointing pivotal metrics for its measurement [2–5].

Community resilience revolves around four cornerstones: robustness, rapidity, redundancy, and resourcefulness [6], as shown in Fig. 1. It's imperative to understand that resilience is an overarching characteristic of communities, extending beyond the individual attributes of buildings or infrastructure components [7,8]. Within these communities, the intertwined nature of components forms a cohesive framework that dictates overall functionality. A disruption or failure in any single component can trigger cascading effects, reinforcing the importance of unity and integration within the community structure [9].

It is often viewed as an attribute of communities as a whole, rather than individual infrastructure components or systems. A resilient community necessitates a resilient built environment comprising various sectors such as residential, commercial, educational, and governmental, all of which are interconnected in maintaining community well-being [7,8]. Therefore, it is essential to consider the interdependence between these building sectors when assessing community resilience [11].

In the aftermath of hazard events, a community's resilience depends not only on the robustness of its building sectors but also on the performance of its transportation system, which significantly impacts the speed of the recovery process. While previous discussions on transportation system performance following hazard events have focused on aspects such as connectivity and travel time, few studies have specifically analyzed the supportive role of transportation systems in the recovery of damaged buildings [12]. However, this is a crucial issue as the repair of damaged buildings relies heavily on the transportation system for the delivery of essential resources, including materials, machinery, and skilled labor [13].

This paper addresses this issue by firstly introducing a method for assessing community functionality that takes into account the interdependence among building sectors, specifically focusing on post-disaster community population capacity or out-migration rate [14], and illustrates it using a simplified model of Beijing, China. We formulate the optimal resilience-driven logistics planning as a sequential optimization

* Corresponding author.
E-mail address: kelvinfkr2015@gmail.com (K. Feng).

https://doi.org/10.1016/j.rcns.2024.05.003
Received 12 March 2024; Received in revised form 22 May 2024; Accepted 24 May 2024
Available online 10 July 2024

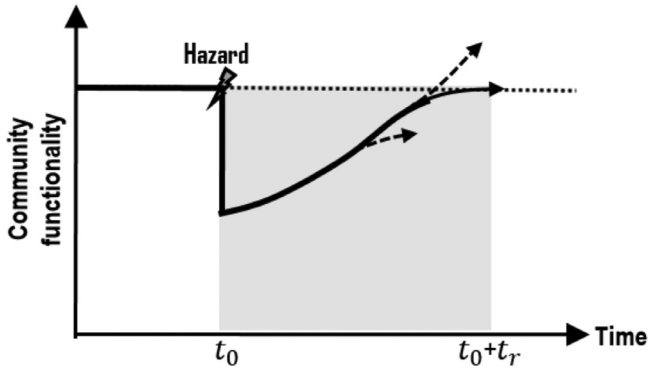

Fig. 1. Schematic representation of community resilience (after [10]).

problem, demonstrating that it can be decomposed into multiple steps, each constituting a capacity-constrained network flow problem.

Additionally, we define an indicator for evaluating the post-disaster performance of transportation systems and introduce a network flow algorithm to determine the optimal logistics plan, thereby facilitating the quickest recovery of community functionality. Finally, through a case study, the paper demonstrates the application of the proposed method and evaluates the supportive role of transportation systems in the recovery of the built environment following an earthquake.

2. Literature review

Building upon the research gap identified in the introduction, this literature review aims to provide a comprehensive overview of the current state of knowledge regarding community resilience and the role of transportation systems in post-disaster recovery. The review is divided into three main subsections, each contributing to the development of the methodology presented in this paper.

The first subsection focuses on historical case studies, examining the impact of past earthquakes on population dynamics and the significance of transportation system recovery in enhancing community resilience. By understanding the lessons learned from these events, we can better inform the development of quantitative metrics for assessing population capacity and outmigration, as well as the strategies for pre-earthquake retrofitting of buildings and transportation infrastructure.

The second subsection explores the various metrics used to assess community resilience performance. By reviewing the evolution of these metrics and their relevance to the current study, we can identify the most appropriate approach for quantifying community functionality and its interdependence with different building sectors. This information is crucial for developing the optimization framework for enhancing post-disaster population resilience.

The third subsection delves into the role of transportation systems in supporting community resilience. By examining previous research efforts and identifying the limitations of existing approaches, we can better understand the need for a more nuanced approach that considers the multifaceted impacts of transportation infrastructure on post-disaster recovery and resilience. This understanding informs the development of the resource supply rate indicator and the application of network flow algorithms to determine the optimal logistics plan for rapid community recovery.

Through this literature review, we aim to establish a solid foundation for the methodology presented in this paper, ensuring that our approach is grounded in the latest research and addresses the identified research gaps effectively.

2.1. Review of historical cases

Drawing lessons from historical seismic events is crucial for understanding their impact on post-earthquake population dynamics and the pivotal role of transportation system recovery in bolstering community resilience. This section reviews key insights gleaned from significant earthquakes in recent history. The 1989 Loma Prieta Earthquake saw basic emergency access restored within hours, with highway repairs ranging from 6 days to 3 months [15]. Rail transit recovery varied, with full restoration taking up to 2 months. Most lifelines were back within 2 weeks, and overall transportation recovery took 2-3 months. The 1994 Northridge Earthquake had major highways reopened within days, with complete functionality restored in 2 weeks [16]. Rail lines took up to 2 months to fully reopen. Lifelines were majorly restored within 3 days, with 95% back in 9 days. Traffic normalized within 6 weeks, and overall recovery was achieved within 1.5-2 months. Ref. [17] studied Kobe's post-1995 earthquake transportation recovery. Major roads were accessible within 24 hours, but complete network recovery took over six months. Rail services faced longer disruptions, with some subway lines taking over two years to fully restore. Traffic in Kobe reached 90% of pre-disaster levels within three months, but full recovery took over six months, which was slower compared to the recovery times observed in the 1989 and 1994 California earthquakes. Following the Kobe earthquake, the city experienced significant resident outflows, primarily consisting of young families and workers, resulting in a population decrease of 50,000-100,000 in the first 1-2 years. By 2000, the population rebounded, nearing pre-quake levels, but an aging demographic persisted. Around 10 years later, the age structure normalized, while fertility rates remained low due to the loss of childbearing groups. By 2010, 15 years post-quake, population growth and composition recovered, as evidenced by census data [18]. The 2008 Wenchuan earthquake severely disrupted transportation, hindering economic and structural recovery [19–21]. Damages included over 100,000 km of highways and 1,500 km of national roads, totaling $2.5 billion in losses. By three months post-quake, only 73% of roads were functional. Railway repairs exceeded $1 billion, with full restoration spanning 3 years. Expressways took up to 18 months to mend, and though airports resumed operations within days, Chengdu airport's full restoration took a year. The Wenchuan earthquake displaced 1.5 million people, with many seeking refuge in other provinces. Over 50% of households in damaged Beichuan city reported out-migration. Analysis of census data revealed a 5%-15% decline in the working-age population in quake-hit regions from 2010-2015, indicating labor migration. By 2012, 270,000 people, mainly migrant workers, had resettled in other provinces due to rebuilding efforts. Many also returned to rebuild by 2015, with over 90% of temporary settlements abandoned. Return migration was spurred by incentives, community ties, and limited prospects elsewhere. By 2020, populations in heavily impacted areas rebounded close to pre-quake levels, as shown by the census data.

2.2. Metrics for assessing community resilience performance

The focus on community resilience became particularly pronounced following the catastrophic impact of Hurricane Katrina on Louisiana, which highlighted the critical need for communities to be able to bounce back from such devastating events. The aftermath of Hurricane Katrina brought to the forefront the concept of population capacity and outmigration as essential metrics for representing community resilience. Historical events have shown that significant outmigration occurs in the aftermath of earthquakes. This shift in focus was due to the observed large-scale displacement and migration of populations affected by the disaster, which underscored the need for resilient communities that can sustain and recover from such shocks. The ability of a community to maintain or quickly resume critical functions and the capacity to absorb, adapt, and recover from a disaster became central themes in resilience research [22–29].

Subsequent research efforts have aimed to quantify the factors impacting population capacity, recognizing that community resilience is influenced by a multitude of factors. Among these, the damage to the built environment and the performance of critical infrastructure have

been identified as key determinants. The extent of damage to homes, businesses, and public buildings directly affects the ability of a community to provide shelter, employment, and essential services, which in turn impacts population capacity and the likelihood of outmigration. Building on these insights, researchers have developed metrics that consider the interaction between different sectors and the damage state of built environments.

Ref. [30] defines resilience in terms of the ability of lifeline systems (e.g., utilities, transportation) to withstand and recover from disruptions, with metrics such as recovery time and service continuity rates. Ref. [31] assesses resilience by the ability to restore critical load supply in power distribution systems post-disaster, incorporating electric bus scheduling as a strategy to optimize the restoration process. Ref. [32] proposes a roadmap for enhancing resilience by quantifying damage rates and recovery times for transportation infrastructure under multiple hazard scenarios. Ref. [33] introduces quantitative measures for assessing the resilience of water distribution systems, focusing on continuity of service, recovery speed, and the system's ability to maintain water supply under disruption. Ref. [34] evaluates resilience through a case study of storm water drainage and road transport, quantifying the inter-dependencies and their impact on system functionality post-hazard. Ref. [35] discusses the resilience of coupled power and water systems, emphasizing metrics such as system robustness, redundancy, and adaptability to ensure uninterrupted services. Ref. [36] focuses on the resilience of coupled urban traffic and electric power systems, using metrics such as traffic flow stability, power supply reliability, and the systems' collective ability to recover from disruptions. Ref. [37] defines resilience as the ability of an interdependent traffic-electric power system to withstand, adapt to, and quickly recover from disruptions, emphasizing the importance of integrated strategies to enhance system robustness and recovery capabilities.

In this study, we adopt the methodology outlined by ref. [14] to develop metrics for quantifying the rate of outmigration following a hazard. This comprehensive approach enhances our evaluation of community resilience by considering the intricate interplay among various building sectors. For instance, our metrics might assess the extent to which damage to commercial infrastructure influences economic activities and healthcare accessibility, thereby impacting the community's overall functionality. Notably, the outmigration rate is among the most established metrics for assessing resilience. Through this perspective, we further distinguish the functionality of the community from its transportation network. This distinction allows us to conceptualize the study in a manner where the transportation system is viewed as a supportive element for community resilience.

2.3. The role of transportation systems in supporting community resilience

By quantifying the factors that contribute to community resilience, policymakers and planners can identify vulnerabilities, allocate resources more effectively, and implement strategies that enhance the community's ability to withstand and recover from future disasters. This includes investments in strengthening critical infrastructure and enhancing emergency preparedness and response capabilities.

The transportation system plays a crucial role in community resilience, serving not only to ensure rapid access to healthcare following disasters but also to facilitate the swift delivery of repair resources to affected areas. The effectiveness of a transportation system's operation can significantly influence its support role in enhancing community resilience. Moreover, the absence of transportation support does not necessarily compromise a community's livability; for instance, if a nearby community remains intact post-disaster, the affected community might still sustain itself and avoid significant outmigration. Therefore, using a single metric to directly describe post-disaster transportation effectiveness may not accurately predict a community's resilience. Hence, research focused on understanding how transportation systems contribute to increasing a community's resilience is required, indicating a need for a more nuanced approach that considers the multifaceted impacts of transportation infrastructure on post-disaster recovery and resilience.

In the past, research on post-disaster transportation systems often focused solely on the recovery of the transportation infrastructure itself. One reason for this is that transportation science primarily emphasizes the restoration speed of transportation equilibrium and the design of transportation systems. Additionally, simulating post-disaster transportation itself poses significant challenges. Another reason is that many studies believe that ensuring the rapid recovery of transportation systems potentially satisfies the demand for maximizing system resilience [38–45]. Ref. [38] utilized a combined effects model to assess seismic performance, focusing on metrics such as system functionality, downtime, and recovery time for urban subway systems. Ref. [39] reviewed various methodologies, including simulation and analytical models, to measure traffic metrics like system reliability, accessibility, and serviceability during disasters. Ref. [40] discussed resilience and vulnerability assessment methods, modeling traffic metrics such as travel time reliability, network capacity, and rerouting flexibility under disruptions. Ref. [41] analyzed transportation network performance using reliability analysis, vulnerability assessment, and resilience quantification, focusing on metrics like network robustness, travel delay, and service level under perturbations. Ref. [42] investigated the role of transportation infrastructure using risk assessment models, emphasizing metrics such as infrastructure damage, functionality loss, and recovery speed post-natural hazards. Ref. [43] coupled mode-destination accessibility with seismic risk assessment, focusing on traffic metrics like accessibility loss, travel disruption, and community isolation to identify at-risk communities. Ref. [44] developed an optimization-based framework for pre-and post-earthquake risk management, modeling traffic metrics related to infrastructure resilience, recovery prioritization, and risk mitigation effectiveness. Ref. [45] developed an agent-based model for post-earthquake analysis of transportation networks, focusing on metrics such as route choice behavior, traffic flow distribution, and network congestion levels to assess and enhance system resilience and recovery strategies.

However, people seldom model the supportive role of the transportation system in resilience based on real resource distribution and operations. This paper seeks to bridge this research void. The paper first introduces a metric for community functionality that considers the interdependency among building sectors, illustrated through a simplified model of Beijing city. Secondly, it defines an indicator for assessing the performance of transportation systems after hazard events. Distinct from connectivity-driven metrics commonly used in other post-earthquake logistics studies, the supply rate encompasses both the damage to the transportation network and the repair requirements for the damaged built environment.Then, a network flow algorithm is introduced to find the optimal logistics plan and the most rapid recovery process of community functionality. Finally, a case study is carried out to demonstrate the application of the proposed method and evaluate the supporting effect of the transportation system on the recovery of the built environment after an earthquake.

3. Methodology

3.1. Quantitative metrics of population capacity and outmigration

The measure of community functionality, as seen in Fig. 1, is required to quantify the community resilience. Conceptually, the community functionality can be defined by the probability of an 'undesired outcome'. In light of this, the degree of population out-migration following a hazard event is chosen as an overall community resilience metric. The occurrence of population out-migration highly depends on the damage conditions of different building sectors, and certain community functionality should be maintained to avoid it [46].

Four essential community functions are considered including housing, business, education and public service, and the buildings supporting each of these four essential community functions are respectively

referred as residential building sector (RBS), business building sector (BBS), education building sector (EBS) and public service building sector (PBS). The community functionality, F_C, which is the potential outmigration rate, is defined as follows[14],

$$F_C = 1 - L_C = 1 - I_{1\times4}[DAM]I_{4\times1} \tag{1}$$

in which F_C and L_C are the overall community functionality and its loss, ranging from 0 to 1; and [DAM] is a *Damage Augmentation Matrix* accounting for the interdependency among the essential functionality provided by the four buildings sectors, which is:

$$[DAM] = \begin{bmatrix} a11 & a_{12}l_1 & a_{13}l_1 & a_{14}l_1 \\ a_{21}l_2 & a_{22} & a_{23}l_2 & a_{24}l_2 \\ a_{31}l_3 & a_{32}l_3 & a_{33} & a_{34}l_3 \\ a_{41}l_4 & a_{42}l_4 & a_{43}l_4 & a_{44} \end{bmatrix} = \begin{bmatrix} 0.13 & 0.30l_1 & 0.37l_1 & 0.27l_1 \\ 0.30l_2 & 0.04 & 0.28l_2 & 0.10l_2 \\ 0.37l_3 & 0.28l_3 & 0.13 & 0.28l_3 \\ 0.27l_4 & 0.10l_4 & 0.28l_4 & 0.05 \end{bmatrix} \tag{2}$$

where l_i is the percentage of buildings in sector i becoming unoccupiable. The threshold value for acceptable functionality, F_C, is 0.87. The detailed derivation for the [DAM] and the threshold of F_C can be found in [14].

It is worth noting that the outmigration rate derived following [14] is based on the assumption that the unoccupiable rate of each sector is relatively small. A complete physical expression of the outmigration rate can be written as: $P_O = \sum p_o(d_1, d_2, d_3, d_4)p_d(d_1, d_2, d_3, d_4)$, where $p_o(d_1, d_2, d_3, d_4)$ represents the probability that a resident will outmigrate when certain sectors are unavailable (for example, $d_1 = 0$ indicating loss of residential buildings), and $p_d(d_1, d_2, d_3, d_4)$ is the probability of a resident being in a situation where some functional sectors are unavailable. An example is $p_o(1, 1, 0, 0)$, which denotes the probability of outmigration when both residential and business sectors are unavailable post-earthquake. By summing over all potential damage states, we obtain a full estimate of the outmigration rate, P_O.

If we assume that the damage probabilities are small, we can neglect higher order probabilities, e.g., $p_d(d_1 + d_2 + d_3 + d_4 > 2) = 0$, which is generally reasonable if the building's earthquake resistance is appropriately aligned with the seismic activity experienced. Under this assumption, P_O only needs to consider second-order interactions between damage states, thereby reducing to a second-order function of the unoccupancy rate. Following this, each variable of DAM can be interpreted with a clear physical meaning as the probability that a resident will outmigrate when some functional sectors are unavailable.

In setting the parameters DAM and the threshold for F_C, we directly follow the approach described in [14], and the calibration conducted in [9]. In their study, four functional states (FSs) Green, Yellow, Orange, and Red are defined for each of these four community sectors employed in this paper. Significant outmigration (PO) was assumed by [9] to occur in scenarios where at least two sectors were in the "Red" state or three or more were in "Orange" or "Red", covering 104 out of the 256 combinations. Following this methodology, Eq. (1) was calibrated by optimizing DAM and F_C values, resulting in a threshold L_C of 13% (i.e., 13% of outmigration), F_C of 0.87 and a corresponding DAM.

3.2. Assessment of seismic performance for building infrastructure and bridges

The relationship between structural response, θ, and seismic intensity, IM, can be expressed in a power-law form [47,48]:

$$\theta = a \cdot IM^b \cdot \varepsilon \tag{3}$$

where a and b are parameters determined by regression analysis and ε is the random error associated with the power-law form. The structural response θ represents the maximum inter-story drift angle (ISDA, in radians) of a moment frame building, b typically varies between 0.8 and 1 when the building period is greater than 1 second. The logarithmic standard deviation of ε, which approximates the coefficient of variation (COV) in θ when IM is known, is typically 0.30-0.40 [49,50].

The fragility value, for an individual building, represents the probability of exceeding a specific limit state; for a group of buildings, it represents the proportion of buildings exceeding the limit state. For building sector i as a whole, the ratio of buildings that are not safe to occupy (l_i) can be written by a log-normal distribution, considering as an average over failure probability of all the buildings of the same type within this community:

$$l_i = 1 - \Phi\left(\frac{\ln(\theta_{cr,i}) - \lambda_{\theta,i}}{\zeta_{\theta,i}}\right) \tag{4}$$

where $\theta_{cr,i}$ is defined as the critical structural response threshold for building sector i, above which the buildings in the sector are considered unsafe to occupy; $\lambda_{\theta,i}$ and $\zeta_{\theta,i}$ can be obtained through simulation-based methods introduced in [10] provided that fragility information on individual buildings in the sector are available. We further define $f_i = 1 - l_i$ as the functionality index of building sector i.

The retrofit cost for sector i, C_i, depending on building characteristics, site conditions and retrofit options, can be determined by a hyperbolic function of retrofitted resistance as follows,

$$C_i = \sum_{i=1}^{n_i} C_{0i} \cdot k_i \cdot \left(\frac{\mu^*_{\theta,i}}{\mu_{\theta,i}} - 1\right) \tag{5}$$

in which C_{0i} is the individual building replacement cost; coefficient k_i is representing the retrofit cost factor associated with the building construction type and site conditions for sector; $\mu^*_{\theta,i}$ and $\mu_{\theta,i}$ are the post- and pre-retrofit mean seismic performance of the building in terms of ISDA computed from Eq. (3). Note that $\frac{\mu^*_{\theta,i}}{\mu_{\theta,i}}$ reflects the improvement in seismic performance by retrofitting.

3.3. Strategies for pre-earthquake building retrofitting

The Cost Efficiency, Z_i, of retrofitting sector i to enhance the overall functionality of the community as a whole is as follows,

$$Z_i = \frac{\partial F_C}{\partial f_i} \cdot \frac{df_i}{dC_i} \tag{6}$$

where

$$\frac{\partial F_C}{\partial f_i} = a_{ii} + \sum_{j=1, j\neq i}^{m} (a_{ij} + a_{ji})l_j \tag{7}$$

$$\frac{df_i}{dC_i} = \frac{df_i}{d\lambda_{\theta,i}} \cdot \frac{d\lambda_{\theta,i}}{d\mu_{\theta,i}} \cdot \frac{d\mu_{\theta,i}}{dC_i} \tag{8}$$

in which m is defined as the total number of building sectors considered in the analysis. Z_i is a key parameter to determine the retrofit strategy, and the building sector associated with the largest value of $Z_i, i = 1, ..4$, has the highest priority for retrofitting.

To enhance community functionality through retrofitting, this framework suggests investing the budget in buildings with the highest cost efficiency until either all funds are allocated or the desired resilience functionality is achieved.

3.4. Optimization framework for enhancing post-disaster population resilience

The earthquake has altered both the capacity and the logistics structure of the transportation network. In response to these changes, a network flow model tailored to handle variations in material flow demand and road capacity has been selected. This model aims to adapt to the altered network dynamics effectively. The overarching goal is to minimize outmigration over a specified period. The rate of outmigration

is represented by $1 - F_C$, indicating that the objective is essentially to maximize the resilience of community functionality, F_C. The objective function and optimization framework without constraint is written as:

$$\max_{NF_t} \int_0^T F_C(t)dt \tag{9}$$

In this context, the time immediately following the earthquake is denoted as 0, and T represents the conclusion of the observed period. The term F_C refers to the functionality of the community over time, which may initially decrease following the disaster but is expected to improve subsequently as repair resources are allocated to each damaged property. The objective of maximization involves considering all possible ways (NF_t) in which resources can be distributed over time, encapsulated by the concept of a temporal network flow.

Directly applying this continuous target poses challenges, particularly when dealing with a finely resolved timeline. At such a granular level, each time point would necessitate an optimal allocation of resources across the transportation network. However, resources newly introduced into the system may not yet have been distributed, potentially obstructing traffic flow. A pragmatic approach to this issue involves discretizing time into larger intervals, such as daily or monthly segments. Under this framework, each road link is assigned a daily capacity limit, preventing the transfer of additional resources once this threshold has been reached. This method simplifies the management of resource allocation by aligning it more closely with the practical limitations of transportation infrastructure and resource distribution logistics.

Then, the optimization target is written as:

$$\max_{NF_0, NF_1, \ldots, NF_T} \sum_0^T F_C(t) \tag{10}$$

Given a network with nodes (V), edges (E), edge capacities ($C_i(u, v)$) at any time i to account for potential damage and subsequent repairs to infrastructure post-earthquake, for each edge (u, v) subject to the following constraints as follows,

(1) *Time-Varying Capacity Constraints*: The flow $nf_i(u, v)$ on any edge (u, v) at any given time i must not exceed its capacity at that time, reflecting the dynamic availability of routes due to damage and repairs:

$$0 \le nf_i(u, v) \le C_i(u, v) \quad \forall (u, v) \in E, \forall i \tag{11}$$

(2) *Conservation of Flow*: For every node, the total incoming flow must equal the total outgoing flow, ensuring that the flow is conserved at each node in the network:

$$\sum_{u:(u,v)\in NF_i} nf_i(u, v) = \sum_{w:(v,w)\in E} nf_i(v, w) \quad \forall v \in V \tag{12}$$

In this section, we have developed an optimization framework to enhance resource logistics. However, the complexity of the problem presents significant challenges in finding a solution. In the subsequent section, we will explore methodologies to address this issue in a numerically feasible manner. Our approach involves two primary strategies:

- *Sequential Piecewise Optimization*: We will demonstrate that by dividing the problem into sequential segments and solving each segment individually, the overall solution remains optimal. This step involves proving that a piecewise approach does not compromise the optimality of the solution, ensuring that the segmented resolution aligns with the global objective.
- *Temporal Reformulation of the Objective*: We will piecewise the objective function to a temporal framework, enabling the application of network flow algorithms. This reformulation is crucial for transforming the problem into one that is more tractable for existing network flow solvers, thereby making the complex optimization problem more manageable.

By employing these strategies, we aim to navigate the complexities of the optimization problem, leveraging the strengths of the network flow framework to achieve a numerically acceptable solution.

3.5. Sequential optimization approach for resilience enhancement

3.5.1. Sequential piecewise optimization

First, we will reformulate the objective function to enable its decomposition into multiple optimization problems, each corresponding to a single time slice. This restructuring is pivotal for simplifying the overall problem into manageable segments. Upon this division, we will demonstrate that each segmented problem exhibits convexity. Leveraging this characteristic, we can apply the theorem stating that the aggregate solution of independent convex optimization problems is separable [51], which is also know as forward Douglas-Rachford splitting scheme [52].

In this section, we reconceptualize the objective function in terms of resources. As previously discussed, the community functionality, denoted by F_C, is influenced by four building sectors. It can be understood as a function reflecting the status of all buildings within the community. Each building's state is represented by a boolean variable b_j. Consequently, F_C is expressed as $F_C(b_1, b_2, \ldots, b_n)$, where n represents the total number of buildings in the community. This formulation allows us to directly link the functionality of the community to the specific condition of each building, facilitating a more granular and effective optimization of resources towards enhancing community resilience.

We proceed by examining the convexity of the community functionality, F_C, with respect to changes in the state of any building, denoted as b_j. Assuming b_j represents a continuous variable, we find that F_C exhibits convexity. This is because F_C fundamentally behaves like a quadratic form, where each b_j reflects the contribution of a building to the overall proportion of functional buildings within its category post-earthquake.

To operationalize this concept within our model, we identify a node $v(b_j)$ that most closely represents the state of b_j. It is posited that repair resources are allocated exclusively to this node. To facilitate the flow of resources within this framework, we introduce the concepts of a virtual sink for resources, denoted as RS, and a virtual source of resources, RR. These entities function as hyper-nodes external to the network E, channeling all resources into the system from RR.

Given the principle of flow conservation, it is understood that all resources eventually converge towards the sink. Each damaged building is linked to the hyper-sink node RS, consuming a unit of resources at each time step. Upon repair, the link connecting the building to the sink is severed, indicating the cessation of resource allocation to that building.

Then, if there is only one specific time step t, the optimization is rewritten as:

$$\max_{NF_t} \Delta F_C^t(b_1, b_2, ..., b_j) = \max_{NF_t} \sum_{j=0}^n \frac{\partial F_C^t}{\partial b_j} \Delta b_j = \max_{NF_t} \sum_{j=0}^n \frac{\partial F_C^t}{\partial b_j} nf_t(v(b_j), RS) \tag{13}$$

subjected to

$$0 \le nf_t(u, v) \le C_t(u, v) \quad \forall (u, v) \in E, \forall t \tag{14}$$

$$\sum_{u:(u,v)\in E} nf_t(u, v) = \sum_{w:(v,w)\in E} nf_t(v, w) \quad \forall v \in V/\{RR, RS\} \tag{15}$$

And all sources, say a total amount of repair resources available for allocation at the given time step of TR, go into RS through buildings, with which

$$\sum_{j=1}^n (1 - b_j) nf_t(v(b_j), RS) = TR \tag{16}$$

This scenario can be recognized as a convex optimization problem, as which basically is linear programming of NF_t. Given that each time slice of the optimization exhibits convexity, and considering that the solutions at any given time point are independentrelying solely on the general state of the current F_C without being contingent on the present

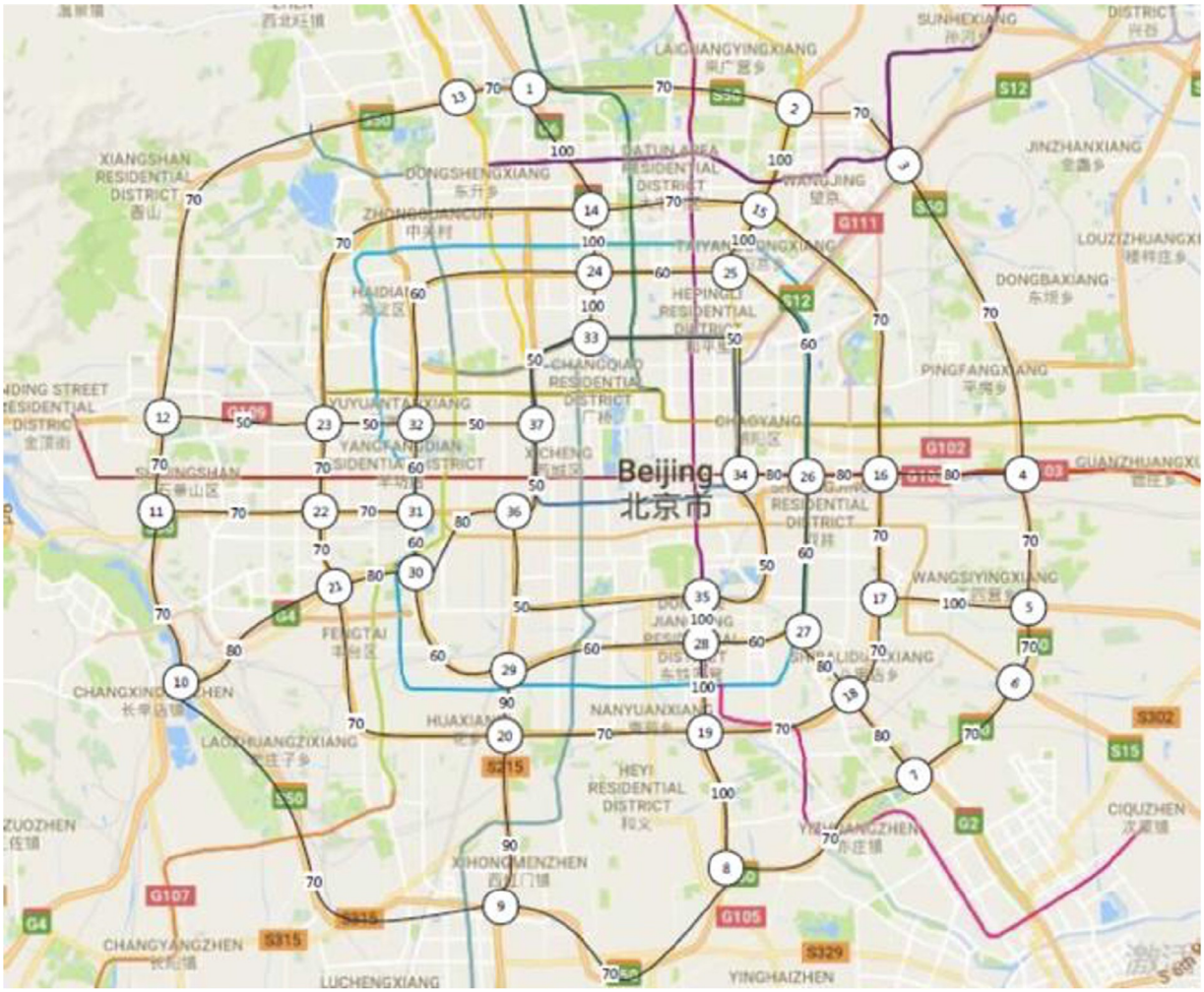

Fig. 2. Map of Beijing city and the simplified logistic network.

decision variablesit follows that employing a forward Douglas-Rachford splitting scheme is effective. According to this scheme, addressing each of these sub-optimization problems in a sequential manner guarantees a globally optimal solution. This methodological approach leverages the inherent convexity and independence of time-sliced optimizations to systematically converge on an optimal configuration for resource allocation and community functionality enhancement over time.

3.5.2. Temporal reformulation of the objective

Upon closer examination of each time slice, it becomes apparent that the problem inherently constitutes a network flow problem[53]. This realization allows for the problem to be solved with a high degree of efficiency, surpassing the speed achievable through traditional linear programming methods. Such efficiency not only facilitates the stochastic simulation of resilience across a multitude of earthquake scenarios, but also empowers us to conduct comparative analyses of the system's resilience under various strategies. These strategies could include, for instance, retrofitting buildings or bridges, thereby enhancing our understanding and approach to improving structural resilience.

4. Example and results

4.1. Description of example

A simplified model of Beijing City shown in Fig. 2 is established to demonstrate the application of the approach, in which four building sectors are considered. Each building sector includes three building categories designed for different seismic intensity levels (SIL), i.e. SIL6, SIL 7 or SIL 8, corresponding to PGAs of 0.06g, 0.13g and 0.25g, respectively. The number of buildings, the seismic response parameters and the basic retrofit costs are shown in Table 1. The building number is estimated from Beijing Municipal Commission of Urban Management[54].

In an effort to streamline our analysis, we initially posit that the majority of buildings within the studied communities, particularly in China, are constructed with reinforced concrete frames. This assumption, while simplifying, aligns with common construction practices observed across various urban settings. The seismic response of these buildings, specifically in terms of inter-story drift, is derived from Eq. (3), where the parameter a is detailed in Table 1 and parameter b is uniformly set at 0.85 for all considered structures [55]. Given the inherent diversity in construction characteristics within any given sector-ranging from variations in building heights and plan dimensions to differences in bay sizes and foundation conditions-it is prudent to model the parameter a as a lognormally distributed random variable, characterized by a coefficient of variation (COV) of 0.3. Through Monte Carlo simulation, we ascertain the mean and standard deviation of the seismic structural response for individual buildings, thereby facilitating the assessment of building category fragility for SIL 6, 7, and 8 within each sector as per Eq. (4). The interrelation of seismic responses among buildings of the same category (e.g., R7, R8, etc.) is estimated with a correlation coefficient of 0.7, aiding in the formulation of a group fragility function for each building category. The resultant fragilities exhibit a COV of approximately 0.7, closely mirroring the COV of 0.75 recommended by HAZUS-MH [56], thereby indicating a higher level of uncertainty for

Table 1
Building sectors and their seismic behaviors.

Building Sector	Building Category	Buildings (in thousand)	a	Design Seismic Intensity Level (SIL)	Retrofit cost per building, $C_0 k$ (billion CNY)
Residential building	R6	40	0.040	6(0.07g)	1.72
	R7	50	0.024	7(0.13g)	1.89
	R8	10	0.013	8(0.25g)	2.06
Business buildings	B6	8	0.046	6(0.07g)	5.15
	B7	10	0.026	7(0.13g)	5.66
	B8	2	0.015	8(0.25g)	6.17
Education buildings	E6	2	0.036	6(0.07g)	2.57
	E7	2	0.021	7(0.13g)	2.92
	E8	1	0.012	8(0.25g)	3.26
Public service buildings	P6	10	0.044	6(0.07g)	0.86
	P7	10	0.025	7(0.13g)	1.03
	P8	5	0.014	8(0.25g)	1.20

building groups compared to the 0.30–0.40 range typically associated with individual structures.

Subsequent to seismic events, buildings are evaluated and categorized into one of five potential damage states-none (< 0.5%), slight (0.5%–1%), moderate (1%–1.5%), severe (1.5%–2%), and collapse (> 2%)-utilizing the ISDA. Following this classification, we assume that buildings with moderate or more damage are deemed non-functional and necessitate repairs before they can be deemed habitable again. It is noteworthy that, when subjected to earthquake intensities surpassing their design specifications-such as a structure engineered for a seismic intensity of 7 (PGA = 0.13 g) experiencing an earthquake of intensity 8 (PGA = 0.25 g)-the likelihood of the building being deemed unsafe for occupancy is approximately 20%. This estimation is in harmony with empirical findings regarding the seismic performance and fragility of extant buildings within China [57]. Accordingly, this study chooses a critical threshold, $\theta_{\mathrm{cr},i}$, at 1%, reflecting a categorization wherein buildings exhibiting either no or slight damage are considered habitable. In terms of restoration, it is estimated that buildings with moderate damage necessitate approximately one month for repairs, those with severe damage require six months, and structures classified as collapsed are deemed to have incurred a permanent loss of functionality.

In our study, we've simplified assumptions to reflect common urban settings, mindful of balancing detail with practicality. Our use of ISDA thresholds for assessing earthquake damage, while standard, may not encompass all nuances. The conservative 1% non-functionality criterion prioritizes safety but may not fit every building type perfectly. Furthermore, our estimated recovery timelines, from one month for moderate damage to considering collapses as permanent losses, aim to provide a framework for planning but could oversimplify the complexities of actual reconstruction. These assumptions are foundational for our analysis, yet we acknowledge they represent a starting point for further refinement and discussion in urban seismic resilience research.

The transporting network in Beijing city is considered in this section, and the study is limited to the 4 ring roads and 10 linking roads, as shown in Fig. 3. This network model consists of 37 nodes and 56 links, and the total number of bridges is 36. The network is defined in terms of nodes and links. A node is at the location where two or more highways intersect (usually interchanges). A link is defined by a line between two nodes with no other nodes in between.

In the context of Beijing city's topology, we initially constructed the graph NF_t, as illustrated in Fig. 3. Here, the source node RR represents a hypothetical node connected to all nodes on the 5th ring, serving as the entry point for all resources transported from other cities to Beijing. Conversely, the sink node RS is another hypothetical node linked to all network nodes, symbolizing the distribution endpoint. The capacity $(C_t(u,v))$ of each edge $(nf_t(u,v))$, is influenced by factors such as average travel speed, number of lanes, and road condition, which collectively determine its designated traffic flow capacity [58]. Fig. 3 displays the normalized daily capacities. It is assumed that every group of one thousand buildings requires five units of resources at each time point to get repaired.

Table 2
Loss in road capacity once the bridge is damaged.

Damage state	None	Slight	Moderate	Severe	Collapse
Capacity loss	0	20%	50%	100%	100%

We assume the damage to bridges to be statistically independent, and the capacity $C_t(u,v)$ is set based on the damage state, as detailed in Table 2, by a ratio relative to the designated traffic flow capacity.

Resource allocation at each node can be modeled through the following steps:

1. Simulate the damage state of bridges and buildings to establish the road system's capacity matrix.
2. Construct the flow network NF_t, incorporating the source node RR and sink node RS into set NF_t, and then assess the cost at each node.
3. Distribute the shipped resources based on the optimal solution derived from network flow analysis, subsequently updating the damage state of each building, revising the node costs, and repeating this step for subsequent daily analyses. This iterative process generates a sample of the city's recovery trajectory.

City transportation system comprises numerous structural components; among them, bridges are the most vulnerable components under earthquake excitations. Similar to the buildings, the bridges of Beijing city were also designed and constructed according to 3 seismic intensity levels. In the previous study [59], bridge fragility information was expressed as a function of peak ground acceleration (PGA), and it was assumed that the curves be expressed in the form of two parameter lognormal distribution function. The fragility curves of bridges of Beijing city is shown in Fig. 4, in which the damage state is classified into 5 categories, i.e., none, slight, moderate, severe and collapse. Once the bridge is damaged, Table 2 shows the loss of traffic capacity depending on the degree of damage.

4.2. Resource supply rate

To evaluate the supporting effect of transportation system to the recovery of built environment, resource supply rate is proposed in this section. For an individual building, the resource supply rate, r_{ind}, is defined as:

$$r_{\mathrm{ind}} = \frac{\Pi_s}{\Pi_n} \tag{17}$$

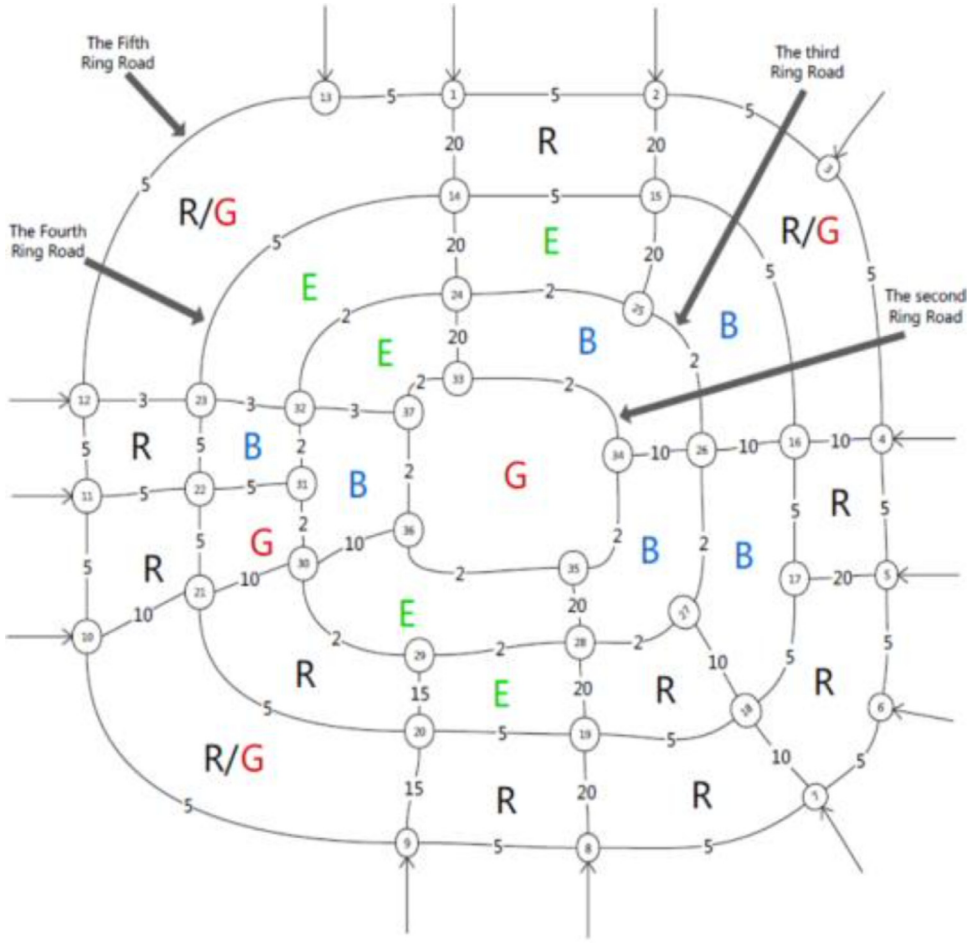

Fig. 3. Map of Beijing city and the simplified logistic network.

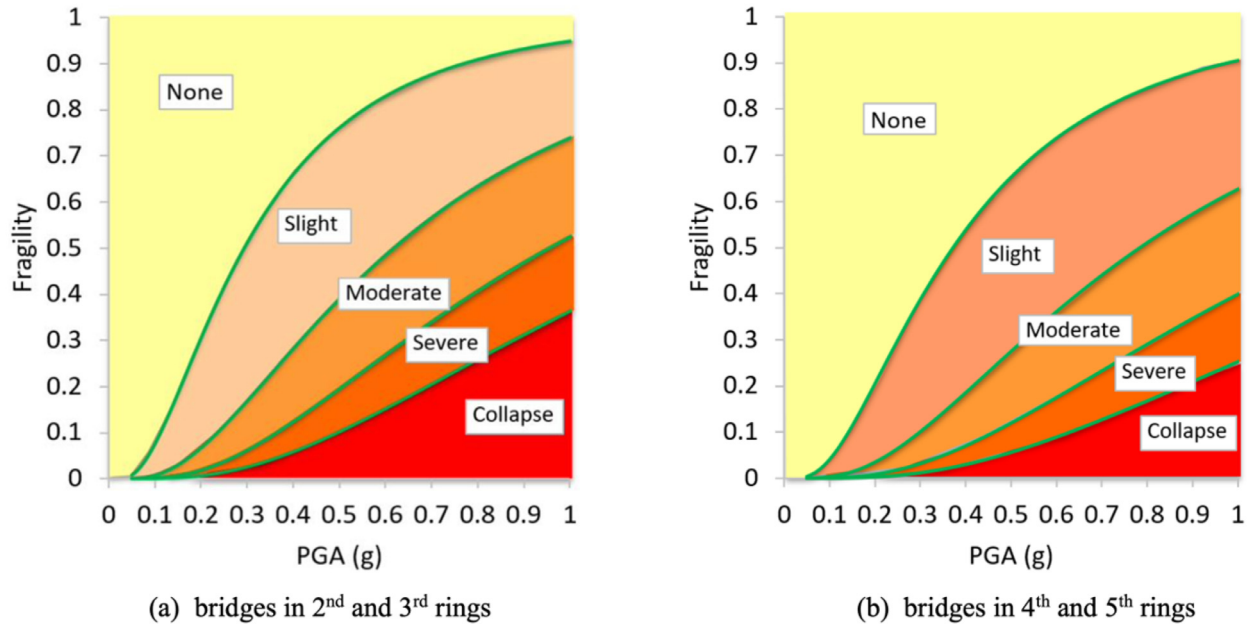

Fig. 4. Fragility curves of Beijing's bridge.

in which Π_n denotes the demanding resources daily for the full speed recovery of the concerned building, Π_s denotes the supplied resources daily to the building through the transportation system. As for the whole community, the resource supply rate, r, is defined as a weighted average of r_{ind} of all buildings in the community

$$r = \frac{\sum_{j=1}^{4} \sum_i w_{ij} r_{ind,ij}}{\sum_{j=1}^{4} \sum_i w_{ij}} \tag{18}$$

in which $r_{\text{ind},ij}$ is the resource supply rate for the i th building in the j th building sector, w_{ij} is the weighting factor, which is determined by:

$$w_{ij} = \frac{\partial F_C}{\partial f_j} \cdot \frac{df_j}{d\Pi_{ij}} \tag{19}$$

in which $\frac{\partial F_C}{\partial f_j}$ distinguishes the importance of different building sector to the functionality assessment of the whole community, and $\frac{df_j}{d\Pi_{ij}}$ reflects the difference in cost efficiency of repairing different individual building in a building sector.

Computationally, for each post-earthquake bridge damage scenario, the resource supply rate can be obtained from the model by following these steps:

- Determine the demanding resources (Π_n) required for the full-speed recovery of each individual building in the community. This information can be based on the extent of damage, building type, and size.
- Calculate the supplied resources (Π_s) that can be delivered daily to each building through the transportation system, considering the damage to the transportation infrastructure and its remaining capacity.
- Compute the resource supply rate for each individual building ($r_{ind,ij}$) using Eq. 17, where i represents the building index and j represents the building sector (e.g., residential, commercial, industrial, or public).
- Evaluate the weighting factors (w_{ij}) for each building using Eq. 19. The term $\frac{\partial F_C}{\partial f_j}$ represents the importance of different building sectors to the overall community functionality, while $\frac{df_j}{d\Pi_{ij}}$ accounts for the variation in cost efficiency of repairing different individual buildings within a sector.
- Calculate the overall resource supply rate (r) for the entire community using Eq. 18, which is a weighted average of the individual building supply rates. This step takes into account the weighting factors determined in the previous step, ensuring that the contribution of each building to the overall supply rate is proportional to its importance and cost efficiency.

The supply rate's spectrum, extending from 0 to 1, provides a nuanced understanding of the disaster recovery process. A value of 0 signifies a complete absence of resources for building repairs, painting a scenario of stalled recovery efforts due to logistical challenges or severe infrastructure damage. Conversely, a supply rate of 1 indicates an optimal scenario where the available resources are sufficient to meet all repair needs, ensuring a swift and efficient recovery process. This ideal state suggests that the transportation system, despite potential damages, retains enough capacity to distribute resources effectively, or that the demand for repairs is low enough to be fully met under the circumstances. From this perspective, it is crucial to strategically assess how well a city's transportation infrastructure aligns with its built environment for earthquake resilience purposes.

4.3. Community resilience assessment and post-earthquake logistics

Having defined the supply rate, we can now initiate a Monte Carlo simulation to analyze post-earthquake resilience, taking into account the constraints imposed by the transportation logistics capability. Assuming an earthquake with a Peak Ground Acceleration (PGA) of 0.25g, which results in damage to buildings and bridges, we conducted 1000 simulated scenarios to assess the damaged state of Beijing's infrastructure. These simulations yielded a collection of recovery trajectories, the probabilities of which are depicted in Fig. 6 using varying shades of color intensity. The shading becomes redder as it approaches the median value, indicating a higher probability, while a lighter shade signifies a lower probability.

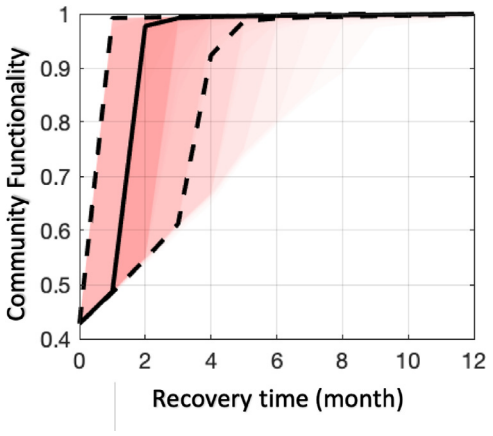

Fig. 5. Recovery trajectories with uncertainty range.

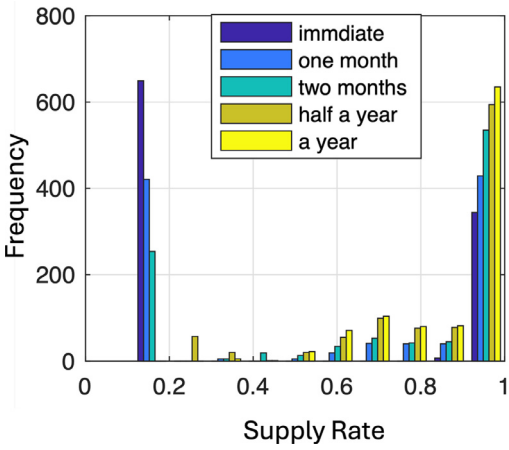

Fig. 6. Probabilistic distributions of resource supply rate at different time.

Fig. 5 features a solid black curve representing the median recovery trajectory, which reveals that, on average, community functionality is restored to an acceptable level (designated as $F_C = 0.87$) within two months. However, the recovery process is subject to significant uncertainty, as demonstrated by the black dashed curves corresponding to the 10th and 90th percentiles. These variations indicate that, in the most favorable scenarios, recovery is rapid, suggesting that with an intact transportation network, resources are sufficiently distributed for prompt building restoration. This finding will be examined in greater detail in the subsequent supply rate analysis.

Conversely, in the least favorable scenarios, recovery could extend beyond eight months before reaching an acceptable level of functionality ($F_C = 0.87$), indicating a protracted period of reconstruction. These results underscore the vast range of outcomes within the simulated recovery processes.

The resource supply rate is also calculated using the simulated results, its probability distribution can be found in Fig. 6. It is a bar graph that illustrates the distribution of supply rates to a city in the aftermath of an earthquake. The graph categorizes the supply rate into five differ-

Table 3
Optimum retrofit strategy under seismic intensity level

	Building Sector	Building Number(in thousand)	Retrofit strategy	Cost (billion)
Residential buildings	R6, R7, R8	100	Not retrofitted	0.00
Business buildings	B6	8	All are retrofitted to seismic level 7	30.96
	B7, B8	12	Not retrofitted	0.00
Education buildings	E6	2	All are retrofitted to seismic level 8	10.95
	E7	2	All are retrofitted to seismic level 8	4.71
	E8	1	Not Retrofitted	0
Public service buildings	P6	10	30% buildings are retrofitted to level 8	7.46
	P7	10	all are retrofitted to level 8	8.21
	P8	5	Not retrofitted	0.00

ent time-frames: immediate, one month, two months, half a year, and a year, suggesting the time elapsed since the earthquake event.

The distribution of the supply rate exhibits two distinct peaks, indicating variability in post-disaster resource efficiency. Specifically, in approximately 30% of the cases, the supply rate approaches 1 immediately after the earthquake, signifying full operational efficiency in resource distribution. Conversely, in about 70% of scenarios, the supply rate is as low as 0.1, indicating a significant reduction in supply efficiency. One month following the earthquake, the supply rate remains at 0.1 for 40% of the cases. This percentage decreases to 25% two months after the event.

Continuing this trend, even after six months, the lowest 5% of cases still experience a supply rate as low as 0.2, highlighting prolonged logistical challenges in certain scenarios. On a more positive note, these results also suggest that there is a considerable probability of achieving a supply rate of 1, where the resources are ample for simultaneous repair of all the necessary buildings, particularly if the transportation infrastructure remains functional after the earthquake. This scenario underscores the importance of robust transportation systems in facilitating efficient post-disaster recovery.

In the next two sections, we will examine methodologies for retrofitting the built environment to bolster the resilience of Beijing City. The first approach involves retrofitting existing buildings prior to an earthquake, while the second addresses the reconstruction of bridges initially designed to lower standards. Subsequently, we will assess and compare the resilience outcomes of these retrofitted scenarios against the original, non-retrofitted cases, focusing on supply rate improvements and economic metrics. To enhance the comparative analysis of the cost-effectiveness of building and bridge reinforcement, we establish a common objective for both retrofitting measures: achieving a median system functionality level of $F_C = 0.87$ within one month post-earthquake after retrofit, which is considered within an acceptable range.

4.4. Influence of pre-earthquake building retrofitting on disaster recovery

For pre-earthquake building retrofitting, our design approach adheres to the investment efficiency determined by Equation 3, followed by a gradual reinforcement of housing stock. For each increment of 0.05 in the initial community functionality (F_C), we conduct a random simulation of a magnitude 8 earthquake's impact on the bridge system (with PGA = 0.25g) and a stochastic simulation of system recovery, continuing until the median system functionality (F_C) reaches 0.87 one month post-earthquake. The optimum retrofit strategy is determined using the proposed method based on cost-efficiency and is presented in Table 3.

Following the most cost-effective pre-earthquake retrofitting of urban buildings, the post-earthquake recovery trajectory is depicted in Fig. 7, where the initial city Functionality Capability (F_C) reaches 0.84. One month after the earthquake, the median city FC rises to 0.88, and within two months, it reaches a median F_C of 1. This represents a significant acceleration in recovery compared to the scenario shown in Fig. 5. In the best-case scenario, the city's F_C could be fully restored within a month. However, in examining the worst-case scenarios, we find that the city still requires 4 to 5 months to return to pre-earthquake functional levels. This suggests that pre-earthquake retrofitting alone may not be sufficient to address all issues regarding community resilience post-earthquake.

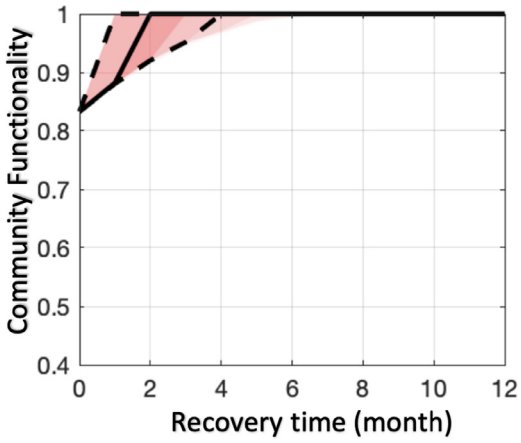

Fig. 7. Recovery trajectories with uncertainty range after build environment retrofit (Similar to Fig. 5).

From an economic perspective, the estimated total cost of retrofitting all buildings in Beijing amounts to approximately 60 billion CNY. This investment could fund the reconstruction of around 300 highway intersections, assuming a retrofitting cost of 0.2 billion CNY per intersection, as derived from [58]. Such funding would more than adequately cover the overhaul of all existing lower-standard highway intersections in Beijing, which number 36 in total. Notably, 23 of these intersections are categorized as having relatively low anti-seismic grades, specifically those located along the 4th and 5th Ring Roads. And 13 with higher anti-seismic grades, located along the 2nd and 3rd ring roads.

4.5. Contribution of pre-earthquake bridge retrofitting to earthquake resilience

Suppose all the bridges are rebuilt to a higher seismic intensity level (this will cost around 7.2 billion), their seismic fragility curves are shown in Fig. 8. Repeating the analyses above, the simulated recovery trajectories are shown in Fig. 9. It can be seen that the time for the built environment back to the acceptable level decreases to 1 months on medium, and the variability of the recovery process is significantly reduced compared with Fig. 5, demonstrating the improvement in the supporting effect of transportation system to the recovery of damaged buildings after the transportation network is retrofitted.

From the recovery curve of community functionality (F_C), we observe that in the majority of scenarios, the city's functionality can be restored to an acceptable level within one month. Even in the worst-case scenarios, recovery to an acceptable level is achievable within two

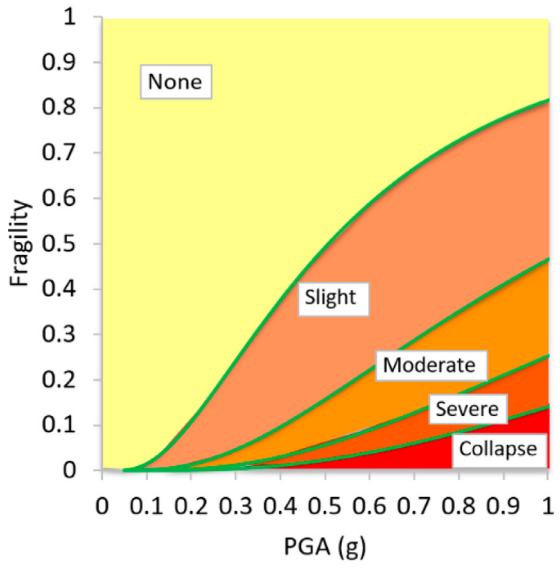

Fig. 8. Fragility curves after retrofitting.

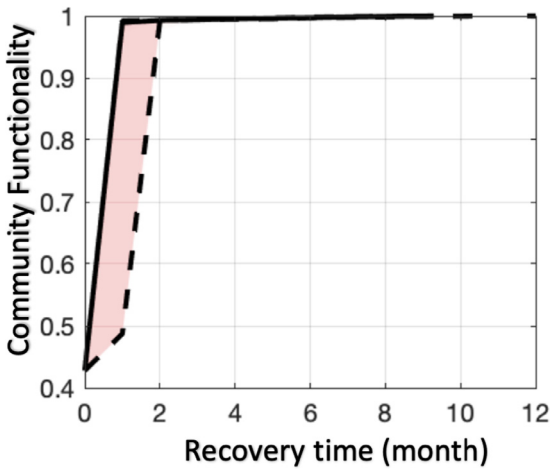

Fig. 9. Recovery trajectories with uncertainty range after transportation system retrofit (Similar to Fig. 5)

months. Overall, the recovery outcomes are slightly better than depicted in Fig. 7. However, due to the lack of building reinforcements, an initial period of low functionality period post-earthquake is inevitable. On the other hand, the transportation system could still suffer significant damage, potentially leading to a two-month period during which the city's functionality remains low.

4.6. *Inter-comparison between three scenarios*

In this section, we compile data on community functionality and supply rate for periods ranging from immediately after the disaster to six months post-event. Community functionality, indicative of a community's capacity to accommodate its population post-disaster, or alternatively, the inverse of the outmigration rate, is examined in Fig. 10. It is evident that one month post-earthquake, cities with either retrofitted buildings or bridges show significant recovery. However, it becomes apparent that the scenario involving building retrofits exhibits much greater uncertainty in resilience compared to bridge retrofits.

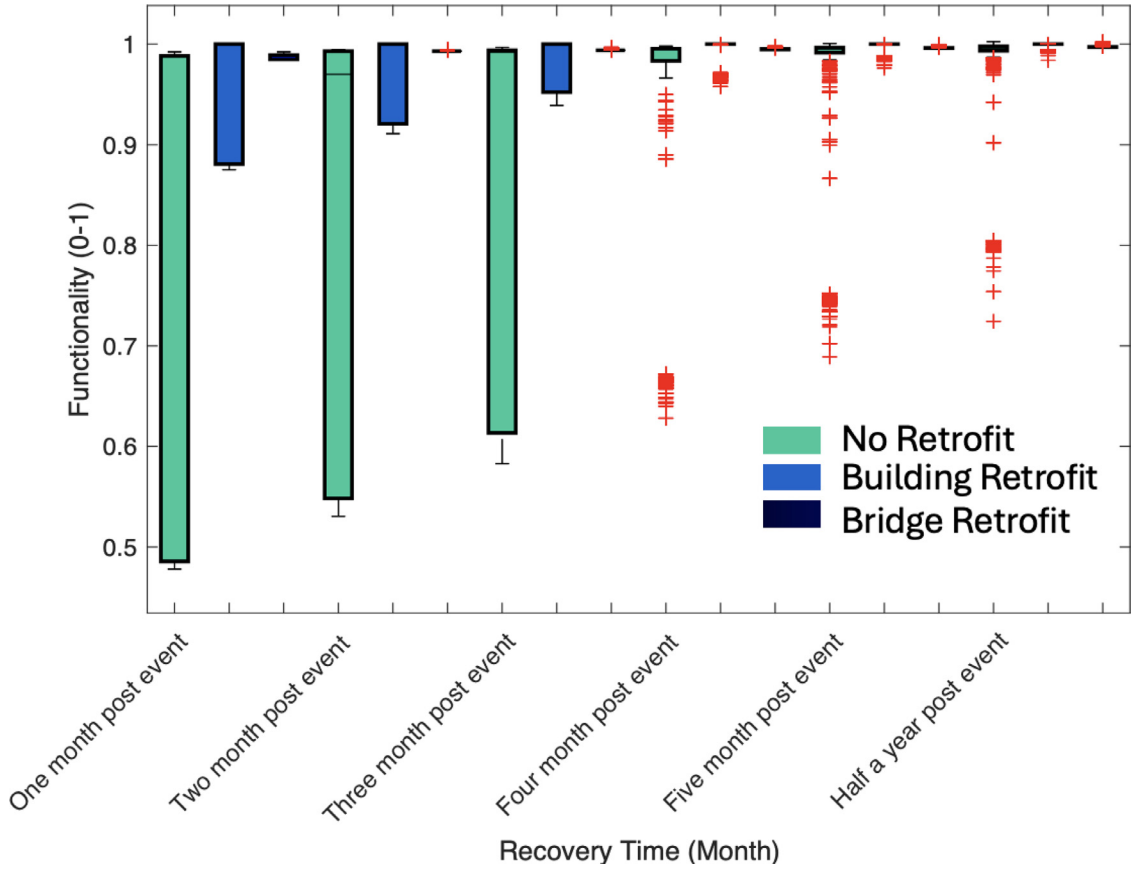

Fig. 10. Sampled recovery trajectories of Functionality.

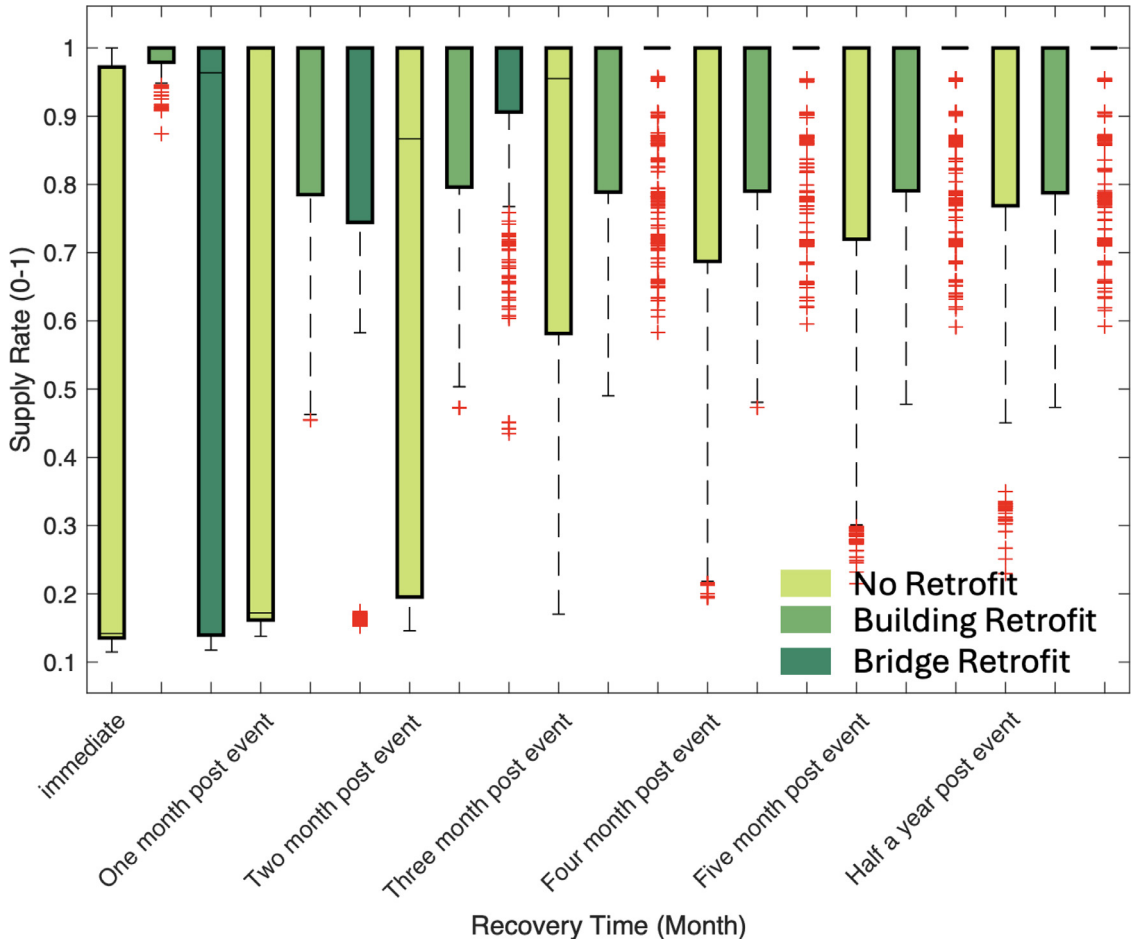

Fig. 11. Sampled recovery trajectories of supply rate.

The supply rate, indicative of the extent to which repair needs can be met, is analyzed in Fig. 11. Immediately following the earthquake, both the non-retrofitted and bridge-retrofitted scenarios exhibit a wide range of supply rates, from 0.1 to 0.9. In contrast, the scenario involving retrofitted building environments achieves a supply rate very close to 1. However, one month later, the supply rate in the building-retrofitted scenario no longer maintains at 1. This decline occurs because the more readily repairable buildings have already been fixed, leaving behind those that are more challenging to repair due to limitations in transportation logistics and bridge damage. Consequently, a relatively low supply rate (approximately 0.9) persists throughout the six months following the earthquake. In the scenario with bridge retrofits, the supply rate swiftly approaches 1 within four months post-event, indicating that most buildings have been repaired. Compared to the baseline scenario (no retrofit), both building and bridge retrofitting significantly enhance the supply rate.

It is important to note that the supply rate merely reflects the proportion of repair demands that can be met and does not guarantee rapid recovery. The rate may not be monotonous; as buildings that are easier to repair are addressed, those remaining are likely to have lower accessibility. Moreover, the analysis reveals that ensuring the traffic system is fully functional post-earthquake can significantly reduce recovery uncertainty and expedite the process.

We can also explore the economic advantages of both building and bridge retrofitting. In the case of Beijing, the cost associated with building retrofitting (60 billion CNY) significantly exceeds that of bridge retrofitting (7.2 billion CNY), even though their resilience performances appear to be quite comparable. However, this comparison may not hold for smaller-scale communities. For instance, in a logistics and transportation hub similar to Beijing, where numerous highways intersect, the expense of bridge retrofitting could remain substantial. Nevertheless, the cost of building retrofitting in such a community might amount to only 10% of Beijing's retrofitting expenses. It's important to note that Beijing's population is 20 million, so a city with 10% of Beijing's population would still have 2 million residents, categorizing it as a large city. In such scenarios, retrofitting buildings could also offer considerable cost efficiency.

5. Concluding remarks and discussion

This study establishes a framework for optimizing logistics in the aftermath of an earthquake. It introduces a novel metric, the supply rate, to assess the functionality of the built environment within a community after a disaster. Additionally, it proposes an indicator to evaluate the capacity of the existing transportation system to support the recovery process. Utilizing practical examples, the effectiveness of both the community functionality metric and the proposed indicator-the resource supply rate of the transportation network-has been illustrated. The results highlight the critical role of the transportation system in aiding the recovery of the built environment, demonstrating the importance of integrating such metrics and indicators in disaster recovery planning and execution.

Additionally, our research emphasizes the importance of aligning the transportation system's capacity to deliver post-earthquake resources with the demand for repair resources. This alignment is vital for establishing resilience-driven design standards or retrofit guidelines aimed at enhancing post-earthquake resilience in urban settings.

In terms of limitations, this study is that it does not utilize actual earthquake data from Beijing, as the city has not experienced a major earthquake in nearly 300 years. Consequently, the analysis is based

on hypothetical scenarios built upon the actual built environment data. However, this does not imply that Beijing is immune to the risk of an magnitude 8 earthquake. In fact, during the 18th year of the Kangxi Emperor's reign (1679), a magnitude 8 earthquake struck Sanhe and Pinggu, causing widespread damage and becoming the largest earthquake in Beijing's history due to its high magnitude and extensive impact. In future research, we plan to calibrate and refine our post-disaster transportation recovery model using real-world events from different regions, ensuring its applicability and robustness across various contexts.

This study also did not account for varying earthquake intensities, which can result in disproportionate damage to buildings and bridges. Consequently, the conclusions may not be universally applicable across different seismic events. Furthermore, our analysis did not address the potential randomness in the transportation system's recovery, assuming uniform repair times for buildings with similar damage states. This simplification overlooks the complexity of stochastic logistical decisions based on specific recovery situations, which could enrich the analysis but would require more nuanced consideration. These would be promising topics for future study. When evaluating the economic metrics for retrofitting the built environment, it is also crucial to consider the incorporation of new building technologies [60,61].

Currently, our pre-earthquake building retrofit strategy focuses solely on the post-earthquake built environment conditions and does not account for the potential benefits that could be derived from support in outer city areas. For example, lower design standards in these areas might still yield benefits from improved logistics. On the other hand, our pre-earthquake bridge retrofit strategy applies a uniform approach to enhance the earthquake resistance of specific types of overpasses. We have not considered using retrofitting as a means to facilitate the recovery process because our current model only addresses a single earthquake scenario and does not encompass a comprehensive life-cycle maintenance study. Considering a life-cycle, full-span design perspective, a more delicate retrofit strategy may enhance the recovery process. This suggests a potential future research direction: developing pre-earthquake retrofit strategies that fully consider the range of potential future events.

The generalizability of our findings is crucial for future studies. While results from Beijing-a major urban and logistical hub-highlight the efficacy of retrofitting strategies, their applicability to other cities may vary due to distinct geographical, infrastructural, and economic characteristics. This variability suggests that retrofitting costs and benefits demonstrated in Beijing might not directly apply to smaller or differently structured urban areas. Consequently, further research is necessary to assess the model's adaptability and the economic and practical feasibility of retrofitting measures in diverse urban settings.

While we discussed the outmigration rate as a major metric representing economic and social factors related to resilience, there are other crucial factors to consider. For example, the living standards of residents who remain in the area post-earthquake could parallel the outmigration rate in importance and merit discussion and management. Future work should include a more comprehensive analysis of cost-effectiveness, potential trade-offs, and long-term benefits of various retrofitting approaches proposed in the paper, moving beyond a single metric for a one-year recovery period.

The relationship between transportation capacity and recovery speed is complex and cannot be fully captured by a single metric. While essential for enabling movement during recovery, transportation capacity alone does not account for variations in logistical efficiency, infrastructure resilience, or pre-existing vulnerabilities. Additionally, factors such as social cohesion and communication infrastructure significantly influence recovery speed. Communities with strong social ties and robust communication networks are often more resilient, mobilizing resources and coordinating responses more effectively.

While this paper primarily focuses on urban areas, it is crucial to address the needs of rural communities in post-earthquake recovery as well. Rural areas often face unique challenges that differ significantly from urban environments, including limited infrastructure, sparse population distribution, and reduced access to emergency services. These factors can hinder effective recovery efforts and prolong the time needed for communities to return to normalcy.

Moving forward, integrating real-time data acquisition and advanced simulation techniques could significantly enhance our understanding of dynamic resilience in urban areas. Merging real-time data, such as traffic flow, bridge and road status, and resource allocation speeds, with simulation models, could lead to more adaptable disaster response strategies. These strategies warrant further discussion in subsequent studies. Additionally, developing decision-support tools that follow the optimization framework of this study is also crucial. These are convincing future research directions.

Relavance to resilience

Our study develops a post-earthquake recovery resources allocation framework and introduces a metric - supply rate - linking transportation capacity to post-earthquake recovery speed, providing a tool for assessing urban resilience. It examines how pre-earthquake measures, like improving building or bridge seismic performance, affect post-earthquake urban population capacity, offering insights into strategies for enhancing built environment resilience. The methodology is applied to Beijing's transportation system, demonstrating how infrastructure improvements can strengthen resilience. The practical application highlights the framework's potential for guiding urban planning and disaster management decisions. Our study emphasizes the importance of retrofitting and strategic investments in built environments and logistical systems to improve urban resilience.

Data and Code Statement

The Matlab code for the numerical framework discussed in this paper is accessible at GitHub (https://github.com/kelvinfkr/Beijing_resilience_logistics), featuring the implementations for network flow analysis and a ranking system for repair sequence prioritization. Additionally, data on network topology and bridge damage states are also available, providing essential resources to help readers compile and fully understand the algorithm.

Declaration of competing interest

We declare no conflicts of interest.

CRediT authorship contribution statement

Kairui Feng: Writing – review & editing, Writing – original draft, Visualization, Validation, Software, Methodology, Investigation, Formal analysis, Data curation, Conceptualization. **Cao Wang:** Writing – review & editing, Writing – original draft, Visualization, Methodology, Formal analysis, Data curation. **Quanwang Li:** Writing – review & editing, Writing – original draft, Visualization, Supervision, Investigation, Formal analysis, Conceptualization.

Acknowledgement

Kairui Feng was partially supported by National Natural Science Foundation of China (Grant No. 62088101). Cao Wang was supported by the Australian Government through the Australian Research Council's Discovery Early Career Researcher Award (DE240100207). These supports are gratefully acknowledged.

References

[1] Zoback ML. "epicenters" of resilience. Science 2014;346(6207). 283–283
[2] Miles SB, Chang SE. Modeling community recovery from earthquakes. Earthquake Spectra 2006;22(2):439–58.

[3] Twigg J. Characteristics of a disaster-resilient community: a guidance note; 2007.
[4] Cutter SL, Burton CG, Emrich CT. Disaster resilience indicators for benchmarking baseline conditions. J Homeland Secur Emergency Manag 2010;7(1):1271–1283.
[5] of Commerce USD, Standards NIO, (US) T. Community resilience planning guide for buildings and infrastructure systems: volume I.&II; 2015.
[6] Bruneau M, Chang SE, Eguchi RT, Lee GC, O'Rourke TD, Reinhorn AM, Shinozuka M, Tierney K, Wallace WA, Winterfeldt DV. A framework to quantitatively assess and enhance the seismic resilience of communities. Earthquake Spectra 2003;19(4):733–52.
[7] Mcallister T. Developing guidelines and standards for disaster resilience of the built environment: a research needs assessment; 2013.
[8] Koliou M, van de Lindt JW, McAllister TP, Ellingwood BR, Dillard M, Cutler H. State of the research in community resilience: Progress and challenges. Sustain Resilient Infrastruct 2020;5(3):131–51.
[9] Mieler M, Stojadinovic B, Budnitz R, Comerio M, Mahin S. A framework for linking community-resilience goals to specific performance targets for the built environment. Earthquake Spectra 2015;31(3):1267–83.
[10] Lin P, Wang N, Ellingwood BR. A risk de-aggregation framework that relates community resilience goals to building performance objectivess. Sustain Resilient Infrastruct 2016;1(1-2):1–13.
[11] Machado-León JL, Goodchild A. Review of performance metrics for community-based planning for resilience of the transportation system. Transp Res Record 2017;2604(1):44–53.
[12] Longstaff PH, Armstrong NJ, Perrin K, Parker WM, Hidek MA. Building resilient communities: a preliminary framework for assessment. Homeland sEcur Affair 2010;6(3):1–23.
[13] Cimellaro GP. Urban resilience for emergency response and recovery. Fund Concept Appl 2016.
[14] Feng K, Wang N, Li Q, Lin P. Measuring and enhancing resilience of building portfolios considering the functional interdependence among community sectors. Struct Saf 2017;66:118–26.
[15] Staff UGS. The loma prieta, california, earthquake: an anticipated event. Science 1990;247(4940):286–93.
[16] Miles SB, Chang SE-L. A simulation model of urban disaster recovery and resilience: implementation for the 1994 Northridge earthquake. Multidisciplinary Center for Earthquake Engineering Research Buffalo, NY; 2007.
[17] Chang SE, Nojima N. Measuring post-disaster transportation system performance: the 1995 kobe earthquake in comparative perspective. Transp Res Part A: Policy Practice 2001;35(6):475–94.
[18] Horwich G. Economic lessons of the kobe earthquake. Econ Dev Cultural Change 2000;48(3):521–42.
[19] Xu P, Lu X, Zuo K, Zhang H. Post-wenchuan earthquake reconstruction and development in china. Disaster Dev: Examin Glob Iss Cases 2014:427–45.
[20] Yang Y, Gao P, Li H. Residents' satisfaction to post-wenchuan earthquake recovery and reconstruction. Natural Hazards 2017;87:1847–58.
[21] Xiang T, Welch EW, Liu B. Power of social relations: The dynamics of social capital and household economic recovery post wenchuan earthquake. Int J Disaster Risk Reduct 2021;66:102607.
[22] Myers CA, Slack T, Singelmann J. Social vulnerability and migration in the wake of disaster: the case of hurricanes katrina and rita. Populat Environ 2008;29:271–291.
[23] Cross JA. Disaster devastation of us communities: long-term demographic consequences. Environ Hazard 2014;13(1):73–91.
[24] West J. Social vulnerability and population loss in puerto rico after hurricane maria. Popul Environ 2023;45(2):8.
[25] Yabe T, Rao PSC, Ukkusuri SV. Regional differences in resilience of social and physical systems: case study of puerto rico after hurricane maria. Environ Plan B: Urban Anal City Sci 2021;48(5):1042–57.
[26] Hu D, Nejat A. Role of spatial effect in postdisaster housing recovery: case study of hurricane katrina. J Infrastruct Syst 2021;27(1):05020009.
[27] Aranda E, Blackwell R, Escue M, Rosa A. Cascading disasters: the impact of hurricane maria and covid-19 on post-disaster puerto rican migrants' adaptation and integration in florida. Latino Stud 2023;21(2):138–61.
[28] Loebach P. Household migration as a livelihood adaptation in response to a natural disaster: nicaragua and hurricane mitch. Popul Environ 2016;38:185–206.
[29] Rosas E, Roberts PS, Lauland A, Gutierrez IA, Nuñez-Neto B. Assessing the impact of municipal government capacity on recovery from hurricane maria in puerto rico. Int J Disaster Risk Red 2021;61:102340.
[30] Kajitani Y, Tatano H. Estimation of lifeline resilience factors based on surveys of Japanese industries. Earthquake Spectra 2009;25(4):755–76.
[31] Li B, Chen Y, Wei W, Huang S, Mei S. Resilient restoration of distribution systems in coordination with electric bus scheduling. IEEE Trans Smart Grid 2021;12(4):3314–25.
[32] Achillopoulou DV, Mitoulis SA, Argyroudis SA, Wang Y. Monitoring of transport infrastructure exposed to multiple hazards: a roadmap for building resilience. Sci Total Environ 2020;746:141001.
[33] Klise KA, Murray R, Walker LTN. Systems measures of water distribution system resilience. Tech. Rep.. Sandia National Lab(SNL-NM), Albuquerque, NM (United States); 2015.
[34] Yang Y, Ng ST, Zhou S, Xu FJ, Li H. Physics-based resilience assessment of interdependent civil infrastructure systems with condition-varying components: a case with stormwater drainage system and road transport system. Sustain Cities Soc 2020;54:101886.
[35] Shinozuka M, Chang SE, Cheng T-C, Feng M, O'Rourke TD, Saadeghvaziri MA, Dong X, Jin X, Wang Y, Shi P. Resilience of integrated power and water systems. Citeseer; 2004.
[36] Fotouhi H, Moryadee S, Miller-Hooks E. Quantifying the resilience of an urban traffic-electric power coupled system. Reliab Eng Syst Saf 2017;163:79–94.
[37] Zou Q, Chen S. Enhancing resilience of interdependent traffic-electric power system. Reliab Eng Syst Saf 2019;191:106557.
[38] Hu J, Wen W, Zhai C, Pei S. Post-earthquake functionality assessment for urban subway systems: incorporating the combined effects of seismic performance of structural and non-structural systems and functional interdependencies. Reliab Eng Syst Saf 2024;241:109641.
[39] Faturechi R, Miller-Hooks E. Measuring the performance of transportation infrastructure systems in disasters: a comprehensive review. J Infrastruct Syst 2015;21(1):04014025.
[40] Mattsson L-G, Jenelius E. Vulnerability and resilience of transport systems–a discussion of recent research. Transp Res Part A: Policy Practice 2015;81:16–34.
[41] Gu Y, Fu X, Liu Z, Xu X, Chen A. Performance of transportation network under perturbations: reliability, vulnerability, and resilience. Transp Res Part E: Logistic Transp Rev 2020;133:101809.
[42] Boakye J, Guidotti R, Gardoni P, Murphy C. The role of transportation infrastructure on the impact of natural hazards on communities. Reliab Eng Syst Saf 2022;219:108184.
[43] Miller M, Baker JW. Coupling mode-destination accessibility with seismic risk assessment to identify at-risk communities. Reliab Eng Syst Saf 2016;147:60–71.
[44] Gomez C, Baker JW. An optimization-based decision support framework for coupled pre-and post-earthquake infrastructure risk management. Struct Saf 2019;77:1–9.
[45] Feng K, Li Q, Ellingwood BR. Post-earthquake modelling of transportation networks using an agent-based model. Struct Infrastruct Eng 2020;16(11):1578–92.
[46] Bruneau M, Reinhorn A. Exploring the concept of seismic resilience for acute care facilities. Earthquake Spectra 2007;23(1):41–62.
[47] Cornell CA, Jalayer F, Hamburger RO, Foutch DA. Probabilistic basis for 2000 sac federal emergency management agency steel moment frame guidelines. J Struct Eng-asce 2002;128(4):526–33.
[48] Li Q, Ellingwood BR. Structural response and damage assessment by enhanced uncoupled modal response history analysis. J Earthquake Eng 2005;9(05):719–37.
[49] Barroso LR, Winterstein S. Probabilistic seismic demand analysis of controlled steel moment-resisting frame structures. Earthquake Eng Struct Dyn 2002;31(12):2049–66.
[50] Luco N, Cornell CA. Effects of connection fractures on smrf seismic drift demands. J Struct Eng 2000;126(1):127–36.
[51] Parikh N, Boyd S. Block splitting for distributed optimization. Math Program Comput 2014;6(1):77–102.
[52] Davis D. Convergence rate analysis of the forward-douglas-rachford splitting scheme. SIAM J Optim 2015;25(3):1760–86.
[53] Edmonds J, Karp RM. Theoretical improvements in algorithmic efficiency for network flow problems. J ACM (JACM) 1972;19(2):248–64.
[54] Beijing Municipal Government. Beijing municipal government departments. https://english.beijing.gov.cn/government/departments/202006/t20200627_1932937.html; 2020. Accessed: 2023-03-09.
[55] Celik OC, Ellingwood BR. Seismic fragilities for non-ductile reinforced concrete frames–role of aleatoric and epistemic uncertainties. Struct Saf 2010;32(1):1–12.
[56] Remo JW, Pinter N. Hazus-mh earthquake modeling in the central usa. Natural Hazards 2012;63:1055–81.
[57] Zhang F-h, Xie L-l, Fan L-c. Study on evaluation of cities' ability reducing earthquake disasters. Acta Seismologica Sinica 2004;17:349–61.
[58] Beijing transportation. https://english.beijing.gov.cn/government/departments/202006/t20200627_1932944.html; Accessed on: 03-09-2024.
[59] Bocchini P, Frangopol DM. Restoration of bridge networks after an earthquake: Multicriteria intervention optimization. Earthquake Spectra 2012;28(2):427–55.
[60] Jia G, Shi Z. A new seismic isolation system and its feasibility study. Earthquake Eng Eng Vib 2010;9(1):75–82.
[61] Jia G, Tabandeh A, Gardoni P. Life-cycle analysis of engineering systems: modeling deterioration, instantaneous reliability, and resilience. Risk Reliab Anal: Theory Appl: In Honor Prof Armen Der Kiureghian 2017:465–94.